Pharmaceutical Research, Vol. 23, No. 3, March 2006 (© 2006)
DOI: 10.1007/s11095-005-9395-x

Research Paper

Enhanced Protein Delivery from Photopolymerized Hydrogels Using a Pseudospecific Metal Chelating Ligand

Chien-Chi Lin[1] and Andrew T. Metters[1,2,3]

Received July 7, 2005; accepted November 3, 2005

Purpose. This study was conducted to investigate the cause of incomplete protein release from photopolymerized poly(ethylene glycol) (PEG) hydrogels and verify the protein-protection mechanism provided by iminodiacetic acid (IDA).
Methods. The *in vitro* release of bovine serum albumin (BSA) from PEG hydrogels prepared under different conditions was studied. Photoinitiator and initial protein concentrations were varied as well as the addition of IDA and metal ions. Protein immobilization within the nondegradable networks via free-radical reaction was demonstrated by gel electrophoresis.
Results. Protein release efficiency was shown to be dependent on photoinitiator and initial protein concentration. Gel electrophoresis results revealed immobilization of protein to the polymer network and further indicated the detrimental role of free radicals in lowering protein-release efficiency. Adding IDA to the prepolymer solution enhanced total protein release from the subsequently photopolymerized network in a dose-dependent manner. The addition of metal ions including Cu^{2+}, Zn^{2+}, and Ni^{2+} further increased BSA release efficiency. Agreement between the protein release data and theoretical model predictions accounting for reversible protein–IDA binding further validated the protection effect provided by IDA and IDA-transition metal complexes.
Conclusions. The protection effect described in this study offers a novel strategy for increasing the delivery efficiencies of many therapeutically valuable proteins.

KEY WORDS: free radical; hydrogel; iminodiacetic acid; photopolymerization; poly(ethylene glycol); protein encapsulation.

INTRODUCTION

Controlled release of bioactive proteins is becoming attractive for disease treatments requiring extended therapeutic effects. Injectable depots of human growth hormone (hGH), for example, are administered in both adults and children to treat chronic growth hormone deficiency (1), whereas slow-acting formulations of insulin are used to prevent hyperglycemia in patients suffering from type I or type II diabetes. Differing from synthetic drugs with small molecular weights, proteins have complex three-dimensional structures and characteristics that provide added challenges for their effective delivery. The correct structural folding determines the bioactivity of a protein and its therapeutic efficiency (2) and therefore must be maintained. Furthermore, environmental factors such as pH, temperature, and solvent composition can have profound effects on the physical stability of a protein (3).

Poly(ethylene glycol) (PEG) hydrogels are excellent carriers for protein delivery because of their high hydrophilicity and aqueous gel-forming environments that help to retain protein stability and bioactivity (4). Furthermore, by altering the composition and the degree of cross-linking, one can readily control the release rate of protein drugs from PEG hydrogels (5). Another advantage of PEG hydrogels is that protein encapsulation and network formation can be achieved simultaneously via *in situ* photopolymerization (6). This provides a convenient and efficient method for loading high concentrations of proteins for subsequent controlled release. The photocuring process is fast, mild, and can be performed under room temperature in aqueous solution. Moreover, spatial and temporal control of the photopolymerization enables hydrogels fulfilling specific physicochemical requirements to be fabricated. Photopolymerization of hydrogels has been applied in tissue engineering (7–11) as well as protein (12–14) and gene delivery (15–17).

The main disadvantage of photopolymerizations comes from the necessary production of highly reactive free radicals that facilitate network polymerization and cross-linking. These free radicals can also induce side reactions between encapsulated protein or DNA and polymer chains during network formation. Quick *et al.* (15–17) used photopolymerized hydrogels for DNA encapsulation and delivery. They

[1] Department of Bioengineering, Clemson University, Clemson, South Carolina 29634, USA.
[2] Department of Chemical and Biomolecular Engineering, Clemson University, 127 Earle Hall, Clemson, South Carolina 29634, USA.
[3] To whom the correspondence should be addressed. (e-mail: metters@clemson.edu)

showed that without the presence of monomer, free radicals attack and damage DNA molecules. Through the use of vitamin C, a radical scavenger, and protamine sulfate, a transfection agent, they were able to preserve the structural integrity of encapsulated DNA (15). These studies suggest that free radicals are responsible for the reduced amount of DNA delivery.

Similar to the DNA damage caused by free radicals, proteins are susceptible to undesirable reactions during polymer network formation that limit protein bioavailability. Research has been conducted in the development of suitable polymeric matrices for protein delivery based on several chemistries including poly(lactide-*co*-glycolide) (PLGA) (18,19), poly (anhydride) (20), and poly(ethylene glycol) (4). However, proteins may still be unstable in these synthetic polymeric matrices because of physical or chemical interactions with the encapsulating network or because of physical or chemical stresses experienced by the protein during matrix fabrication and protein encapsulation. Previous studies focused on PLGA delivery systems show that proper protein stabilization strategies are needed to increase the delivery efficiency and bioactivity of encapsulated proteins (21–28). However, a protein stabilization strategy to overcome free-radical-induced protein–polymer reactions has not been discovered. Reactions with free radicals can reduce the bioactivity and bioavailability of the encapsulated protein. The decreased total protein delivery is attributable to protein denaturation, aggregation, or conjugation to the polymer network.

It is well known that recombinant proteins with polyhistidine tags on their N- or C-terminals can be easily purified by using immobilized metal ion chelating affinity chromatography (IMAC) (29–31). It has been shown that histidine residues offer the strongest interaction with chelators such as nitrolotriacetic acid (NTA) (32–35) or iminodiacetic acid (IDA) (36–38) in the presence of divalent transition metal ions including Cu^{2+} and Ni^{2+}. In particular, the three-amino-acid sequence Asp–Ala–His on the N terminus of bovine serum albumin (BSA) is the strongest binding site for copper ions (39–42). The strong binding between BSA and the chelator–metal ion complex is associated with the deprotonated Asp–Ala (43). We hypothesize that the same mechanism is responsible for the reaction between protein and the monomeric or polymeric free radicals during photopolymerization. Therefore, when highly reactive free radicals are generated from photoinitiators, reactions with the deprotonated amide on BSA may occur and form protein–polymer conjugates, which result in permanent, irreversible changes to the protein chemistry, structure, and bioavailability.

To increase the delivery efficiency of BSA from photopolymerized networks, the factors affecting total protein release from nondegradable PEG hydrogels are evaluated as part of this study. A strategy for protecting BSA from free-radical reaction during polymer network formation and protein encapsulation is proposed by adding a known protein-binding ligand, IDA, to the prepolymer solution. BSA–IDA binding should minimize the exposure of highly reactive N-terminal residues of BSA to the free radicals generated during hydrogel formation. BSA was chosen because of its known affinity to both IDA and IDA–metal ion complexes. Nondegradable PEG hydrogels are used to eliminate any release due to gel degradation. A theoretical model for estimating total protein release efficiency is derived based on the equilibrium dissociation constant (K_d) of the protein–IDA complex.

MATERIALS AND METHODS

Formation of Protein-Loaded PEG Hydrogel

PEG diacrylates (PEGDA) were synthesized by reacting linear 3.4 kDa PEG (Sigma-Aldrich) with acryloyl chloride (Sigma-Aldrich) as described elsewhere (44). PEG hydrogels were formed via solution photopolymerization of PEGDA monomers. Briefly, PEGDA macromer was dissolved in 50 mM, phosphate-buffered solution (PBS, pH 7.4) to a concentration of 10 wt.%. Required stoichiometric amounts of BSA (Sigma-Aldrich), IDA (Fisher Scientific, Pittsburgh, PA, USA), and metal ions including cupric sulfate pentahydrate, zinc sulfate heptahydrate, or nickel sulfate hexahydrate (Fisher Scientific) were mixed with PEGDA precursor solutions. Prior to photopolymerization, Irgacure 2959 (I-2959), a photoinitiator, was also added at the desired concentration. A portion (50 μL) of the mixed precursor solution was injected between glass slides separated by 0.8-mm Teflon spacers and was exposed to a 100-W UV lamp (BLACK-RAY®) with a maximum intensity of 8.4 mW/cm^2 at 365 nm for a total of 20 min.

In Vitro Protein Release

PEG hydrogels (weight, ~50 mg) loaded with BSA, with or without chelating ligands, were placed into 5 mL PBS (pH 7.4) for *in vitro* protein release at 37°C. At specified time intervals, 200-μL supernatant solutions were sampled and replaced with an equal amount of fresh PBS. The cumulative percent of protein released was quantified by a fluorescamine assay. Briefly, fluorescamine (Sigma-Aldrich, St Louis, MO, USA) was dissolved in acetone to a final concentration of 3 mg/mL. A portion (150 μL) of the sample solution was mixed with 50 μL fluorescamine solution for fluorescence quantification at an excitation wavelength of 395 nm and an emission wavelength of 475 nm using a microplate reader (Spectramax GeminiEM, Molecular Devices, Sunnyvale, CA, USA). Protein concentrations in measured samples were quantified using the linear portion of a standard fluorescence curve constructed from solutions of known concentrations.

Nonreducing SDS-PAGE Experiments

The effect of free-radical-induced BSA immobilization to PEG monomers was examined by SDS-PAGE. Linear 3.0-kDa PEG monoacrylate (PEGMA) was used to replace PEG3400 diacrylate to prevent photocrosslinking and gel formation during photopolymerization of samples. The amount of PEGMA used in these experiments was calculated based on the same concentration of acrylate bonds present during hydrogel formation and protein encapsulation. Varying amounts of IDA or IDA–Cu^{2+} complex were added. The samples prepared for SDS-PAGE were loaded without any denaturation treatments so that any changes in the molecular weight or conformation of the BSA molecules could be detected.

Swelling Ratio Measurements

The swelling ratios of PEG hydrogels were measured to characterize the gel cross-linking density. After photopolymerization, gels were placed into an excess amount of PBS (pH 7.4) for swelling. Gels were allowed to swell for 2 days to reach equilibrium and then dried completely under reduced pressure at room temperature. Gel weights before and after drying were taken and the mass swelling ratios (Q) were determined by the following equation:

$$\text{Swelling Ratio}(Q) = \frac{\text{Swollen Weight}}{\text{Dried Weight}}$$

Theoretical Model of Protein Release Efficiency

The affinity between BSA and metal ion charged ligands such as iminodiacetic acid is well documented (36). The binding of IDA to BSA is believed to reduce the protein–polymer conjugation caused by free radicals produced during network formation and thus increase the total amount of protein released from PEG hydrogels. In the model development, two assumptions were made: (1) BSA has only a single binding site for IDA–Cu^{2+}, and (2) BSA is released in a nonaggregated state. The shielding effects provided by IDA and various IDA–metal ion complexes were modeled by assuming a reversible association between the two components given by:

$$\text{Protein} + \text{Ligand} \overset{K_d}{\longleftrightarrow} \text{Protein} \cdot \text{Ligand Complex} \qquad (1)$$

The dissociation constant (K_d) of the protein–ligand interaction can be expressed by the following equation:

$$K_d = \frac{[P][L]}{[P \cdot L]} = \frac{([P]_0 - x)([L]_0 - x)}{x} \qquad (2)$$

where $[P]_0$ and $[L]_0$ are the initial concentrations of protein and ligand in the precursor solution and x is the concentration of associated protein, ligand, or protein–ligand complex.

The dissociation constants for BSA–IDA and BSA–IDA–Cu^{2+} are 0.4 and 0.0082 mM (43), respectively. By knowing K_d, Eq. (2) can be used to determine $x/[P]_0$, the fraction of protein bound to the ligand at equilibrium, for any combination of $[P]_0$ and $[L]_0$. Increasing the ligand–protein ratio or decreasing K_d shifts the equilibrium such that a greater fraction of protein is present in the bound or "protected" form.

Furthermore, total release (T_R) is defined as the percentage of protein released after an infinite amount of time compared to the amount initially present in the gel and can be expressed as:

$$T_R = \frac{[P]}{[P]_0} \times 100\% = \frac{[P]_0 - i([P]_0 - x)}{[P]_0} \times 100\%$$
$$= \left\{1 - \frac{ixK_d}{([L]_0 - x)[P]_0}\right\} \times 100\% \qquad (3)$$

where i is the fraction of immobilized protein obtained when no ligand is present during gel formation. i is obtained by experimentally measuring total protein release (T_R) when $[L]_0 = 0$ and is equivalent to (100% − T_R) under these conditions. Therefore i accounts for any nonspecific adsorption of protein to the polymer network as well as the presence of any aggregated protein that cannot be released. All other parameters needed to solve Eq. (3) are determined *a priori* based on ligand selection and composition of the gel precursor solution.

RESULTS AND DISCUSSION

Photoinitiator Effects on BSA Total Release

Several critical factors lead to incomplete release of proteins encapsulated during hydrogel photocuring. These factors can be either directly or indirectly related to the free-radical induced cross-linking in the hydrogels. Under UV exposure, free radicals generated from photoinitiators propagate through the vinyl bonds on diacrylated PEG molecules and form cross-linked hydrogels. However, if other reactive sites on protein surfaces are present during photopolymerization, free radicals will also propagate through these sites. Although the exact mechanisms of interaction between these free radicals and encapsulated proteins remains unresolved and most likely varies dramatically with protein surface chemistry, we hypothesize that these interactions lead to the irreversible immobilization of proteins within the hydrogel networks.

The most apparent variable affecting free radical concentration is the photoinitiator concentration. Excessive amounts of free radicals generated from photoinitiators play a critical role in limiting the bioactivity and bioavailability of encapsulated objects such as DNA, proteins, and cells. As shown in Fig. 1, incomplete release of BSA from photocured gels is observed at every photoinitiator (I-2959) concentration. As higher photoinitiator concentrations produce higher concentrations of free radicals during UV irradiation, a greater number of undesirable protein–radical interactions and a lower total release of BSA is expected as I-2959 concentration increases. This trend is confirmed by the

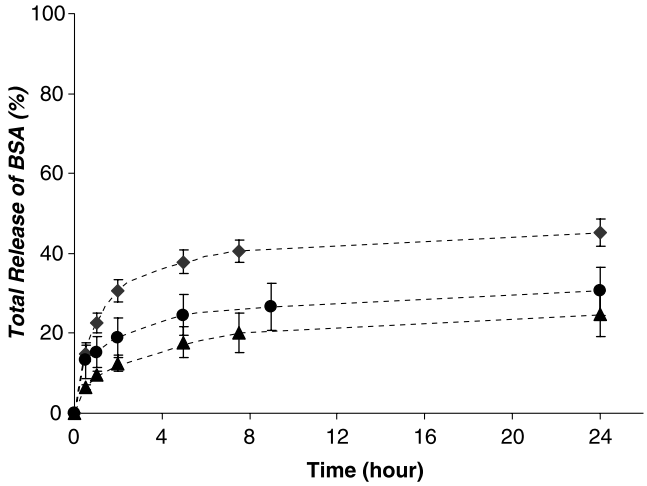

Fig. 1. The effect of photoinitiator concentration on BSA release. BSA (5 wt.%) released from 10 wt.% PEGDA hydrogels polymerized with 0.2 wt.% (♦), 0.5 wt.% (●), and 1.0 wt.% (▲) of photoinitiator (I-2959) (n = 3, mean ± SD).

experimental results in Fig. 1, which show that total release of BSA decreases from 42 to 21% after 24 h as the concentration of I-2959 is increased from 0.2 to 1.0 wt.%.

The decrease in BSA release with an increase in photoinitiator concentration cannot entirely be attributed to changes in gel cross-linking density. The hydrogel mass swelling ratio decreases slightly and reaches a plateau with increasing initiator concentration (7.43 ± 0.16, 6.64 ± 0.28, and 6.75 ± 0.34, respectively for hydrogels cured with 0.2, 0.5, and 1% photoinitiator). Furthermore, based on the release profiles, the diffusivities of releasable BSA within the gels of varying initiator concentration were found to be identical (~1.0×10^{-7} cm^2/s). These results suggest that the decrease in the total release of BSA with initiator concentration is a result of increased protein–polymer coupling rather than changes in gel swelling.

To further investigate the cause of incomplete release, the total release of BSA from photopolymerized PEG hydrogels loaded with different concentrations of BSA was studied. The results in Fig. 2 indicate that total release of BSA is also a function of initial protein concentration. When BSA is initially loaded at 15 wt.%, over 80% of the protein is released within 24 h. However, less than 50% of the protein is released when BSA is loaded at 5 wt.%. Therefore, the absolute amount of released protein increases with initial protein concentration. It is interesting to note, however, that the amount of unreleased protein within each of these networks remains relatively constant as can be seen in Table I. This observation is attributed to the fact that all of these networks were photopolymerized under identical conditions (photoinitiator concentration, light intensity, etc.) and thus should present the same concentration of free radicals to encapsulated BSA during hydrogel formation.

BSA–Polymer Conjugation

The structural integrity of BSA was examined by SDS-PAGE to demonstrate the coupling of BSA with PEG macromers via free radicals during photopolymerization (Fig. 3). The rationale for choosing SDS-PAGE instead of other molecular weight determination techniques such as MALDI-TOF is that the polymerization process yields protein–polymer conjugates with a wide distribution of molecular weights because of the polydispersity of the photopolymerized polymer chains. PEG monoacrylate (PEGMA, M_W = 3,000 Da) is used instead of PEGDA to prevent gel formation and allow sample elution on the PAGE gel.

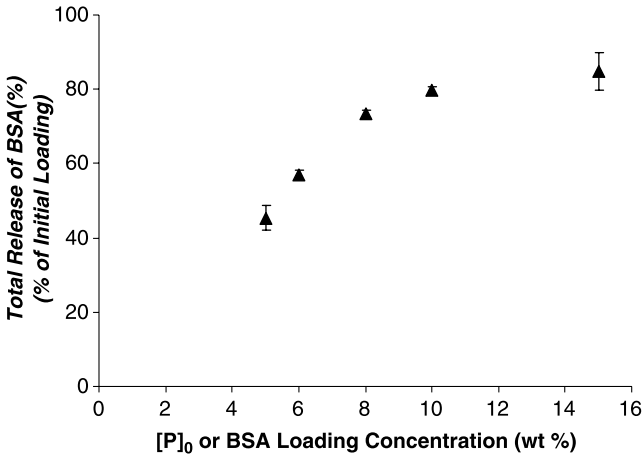

Fig. 2. The effect of BSA initial loading concentration on its total release. Different amounts of BSA (wt.%) were loaded into 10 wt.% PEGDA gels. n = 3, mean ± SD. Concentration of I-2959: 0.2 wt.%.

Table I. Total Amount of Released and Unreleased BSA From Photopolymerized PEG Networks as a Function of Protein Loading (n = 3, Mean ± SD)

Concentration of loading BSA (wt.%)	Amount of loaded BSA (mg)	Total release of BSA (%)	Amount of unreleased BSA (mg)
5	10	51 ± 3.0	4.9 ± 0.3
6	12	55 ± 0.7	5.3 ± 0.1
8	16	73 ± 1.4	4.3 ± 0.2
10	20	80 ± 1.0	4.1 ± 0.2
15	30	85 ± 5.0	4.6 ± 1.5

Photoinitiator Induced BSA–Polymer Conjugation

As shown in Fig. 3a, when BSA and PEGMA are subjected to free-radical-induced photopolymerization, broad distributions of higher molecular weight products were produced, suggesting that a large portion of the encapsulated BSA is covalently bound to polymerized oligomers of PEG. This results in higher molecular weight products (lanes 5–7) compared to native BSA (lane 1). When higher concentrations of I-2959 were added to the protein–polymer mixture and subjected to UV exposure, the fraction of unmodified BSA monomer was decreased. Assuming any modified protein would not be released from a cross-linked polymer as a result of its immobilization onto the network, this result agrees with the release trends of Fig. 1 that demonstrate decreased BSA release with increasing photoinitiator concentration. This phenomenon clearly demonstrates the significant structural modification of BSA that occurs only in the combined presence of photoinitiator, monomer, and UV light.

Polydispersity of BSA–Polymer Conjugates

The broad distributions of BSA molecular weight products that occur during free-radical photopolymerization (lanes 5–7 in Fig. 3a) are due to the high polydispersity (PDI) of the conjugated PEG chains. BSA was conjugated onto uncross-linked PEG molecules that polymerize with a high polydispersity, leading to a broad distribution of high molecular weight products. Therefore, no specific bands at molecular weight above monomeric BSA (M_W ~60 kDa) are seen. Without UV exposure, BSA remains unmodified with the presence of I-2959 and PEGMA (lane 2). Also, when BSA and I-2959 (lane 3) or BSA and PEGMA (lane 4) were subjected to UV exposure, no molecular weight modification was found in either case. This suggests that all three components are required for free-radical induced protein–polymer conjugation to occur.

BSA Aggregates

As shown in lane 1 of Fig. 3a, an extremely small amount of BSA dimers, trimers, and aggregates appear above monomeric BSA (120, 180 kDa, etc). Furthermore, Fig. 2 indicates that the total BSA release increases with initial BSA concentration. Combining these results with Fig. 3a suggest that aggregates do not contribute to the fraction of unreleased BSA in the hydrogel systems studied. The results in lanes 5–7 reveal that even relatively stable proteins such as BSA are modified under standard photopolymerization reaction conditions. Therefore, proper protein stabilization strategies are needed when encapsulating proteins into photopolymerized hydrogels.

Ligand-Mediated Protein Protection

The ligand-mediated protection effect of BSA protein is directly demonstrated in Fig. 3b. The addition of IDA (Lane 3) or IDA-Cu^{2+} complex (Lane 4) prevents the polymerization of BSA molecules with PEG3000MA macromers as indicated by the absence of any significant molecular weight modification. This result qualitatively supports our hypothesis of IDA-mediated protein protection.

Effects of Metal Chelating Ligand on BSA Total Release

Enhanced protein delivery is achieved by adding IDA to the prepolymer solution prior to photopolymerization. As shown in Fig. 4, the total release of BSA is increased from about 40% to 60% when IDA is added in a molar ratio of 0.5 (to BSA). Total BSA release is further increased to almost 70% when IDA/BSA molar ratio is increased to 1.0.

Adding transition metal ions such as Cu^{2+} can further increase the affinity between BSA and IDA. The coupling of Cu^{2+} to metal ion chelators such as IDA has been well studied in the field of immobilized metal ion chelating affinity chromatography (IMAC). The dissociation constant of IDA–Cu^{2+} and BSA coupling is 0.0082 mM (45) compared to a value of 0.4 mM for the coupling of IDA and BSA. In other words, IDA–Cu^{2+} has a greater affinity for BSA than IDA alone. As shown in Fig. 5, although the BSA/IDA molar ratio is held constant at 1, total BSA release increases as more Cu^{2+} ions are added. When Cu^{2+} is added in a molar

A

	1	2	3	4	5	6	7
I-2959	–	+ 0.2 %	+ 0.2 %	–	+ 0.2 %	+ 1.0 %	+ 4.0 %
PEGMA	–	+	–	+	+	+	+
UV	–	–	+	+	+	+	+
IDA	–	–	–	–	–	–	–
Cu^{2+}	–	–	–	–	–	–	–

B

	1	2	3	4
I-2959	–	+ 0.2 %	+ 0.2 %	+ 0.2 %
PEGMA	–	+	+	+
UV	–	+	+	+
IDA	–	–	+	+
Cu^{2+}	–	–	–	+

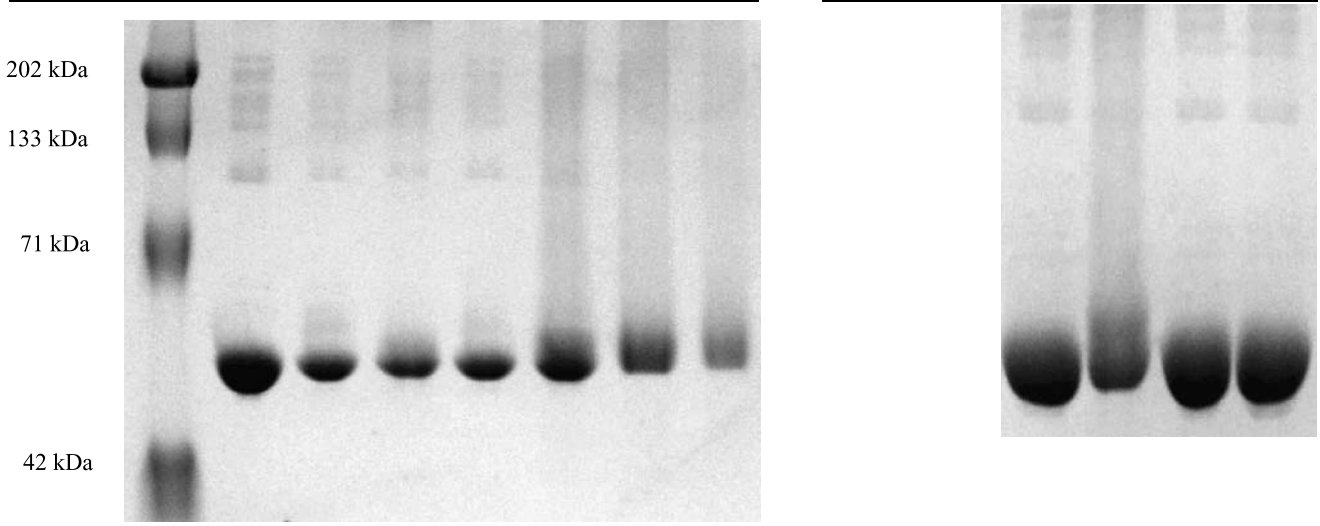

Fig. 3. The determination of BSA structural integrity using SDS-PAGE. A significant amount of higher molecular weight products appear when BSA is mixed with PEG3000MA and photoinitiator (I-2959) and exposed to 365nm UV light for 20 minutes. (**A**) Lanes: (1) Native BSA; (2) 5 wt% BSA, 0.2 wt% I-2959 and PEG3000MA without UV exposure; (3) 5 wt% BSA and 0.2 wt% I-2959 subjected to UV exposure; (4) 5 wt% BSA and PEG3000MA subjected to UV exposure; (5) 5 wt% BSA, PEG3000MA and 0.2 wt% I-2959 subjected to UV exposure; (6) BSA, PEG3000MA and 1.0 wt% I-2959 subjected to UV exposure; (7) BSA, PEG3000MA and 4.0 wt% I-2959 subjected to UV exposure. (**B**) Lanes: (1) Native BSA; (2) 5 wt% BSA, PEG3000MA and 0.2 wt% I-2959 subjected to UV exposure; (3) 5 wt% BSA and molar equivalent of IDA, PEG3000MA, and 0.2 wt% I-2959 subjected to UV exposure; (4) 5 wt% BSA and molar equivalent of IDA-Cu^{2+}, PEG3000MA, and 0.2 wt% I-2959 subjected to UV exposure.

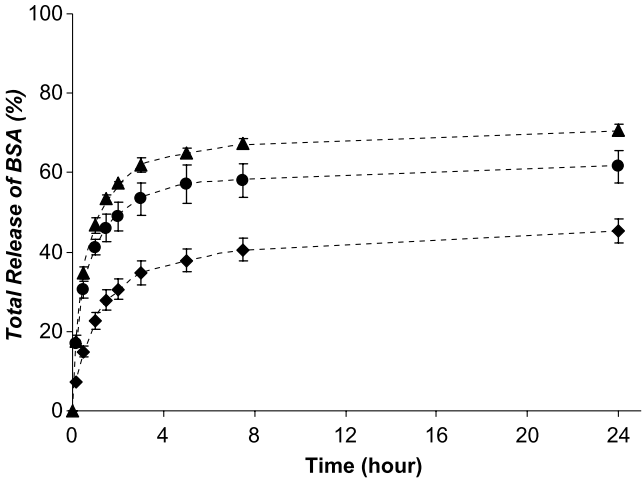

Fig. 4. The effect of IDA concentration on BSA total release. BSA (5 wt.%) was mixed with PEGDA (10 wt.%) and IDA in molar ratios (IDA/BSA) of 1 (▲), 0.5 (●), and 0 (♦) in the prepolymer solution and released from PEGDA hydrogels. $n = 3$, mean ± SD. Concentration of I-2959: 0.2 wt.%.

ratio of 1, the total release of BSA is increased to almost 100%. No significant increase in total release is observed when Cu^{2+} is added to the prepolymer solution without IDA present (data not shown).

Metal Ion Effects on BSA Total Release

From IMAC studies, it is well known that the affinity between protein and ligand can be varied by using different transition metal ions (46–48). For example, Cu^{2+} provides the strongest binding affinity to BSA, followed by Ni^{2+} and Zn^{2+} (48). Ideally, at the same IDA concentration, BSA release efficiency should increase with protein–ligand binding strength. As shown in Fig. 6, the total release of BSA increases when Zn^{2+} or Ni^{2+} are added along with IDA, compared to adding IDA alone. Furthermore, total release is even higher when Cu^{2+} ions are added and approaches 100%.

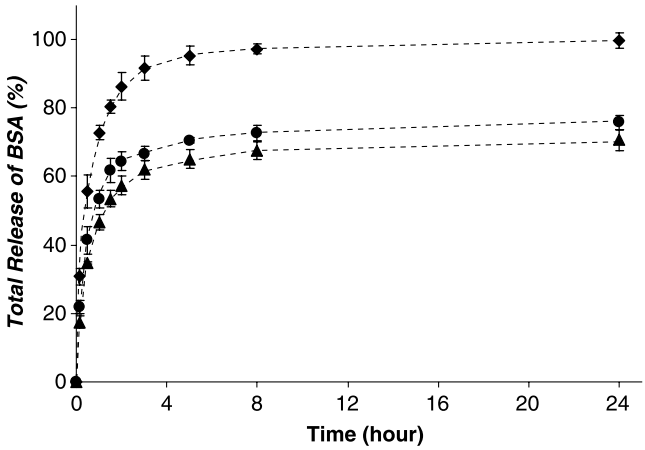

Fig. 5. Effect of Cu^{2+} concentration on BSA total release. BSA (5 wt.%) was mixed with PEGDA (10 wt.%), IDA, and different amounts of Cu^{2+} ions. Molar ratio of IDA to BSA is held at 1. Molar ratios of Cu^{2+} ions to BSA are 1 (♦), 0.5 (●), and 0 (▲). $n = 3$, mean ± SD. Concentration of I-2959: 0.2 wt.%.

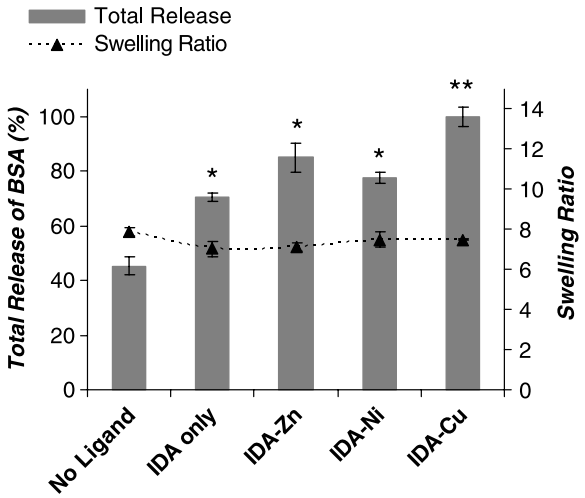

Fig. 6. The effect of different metal ions on total BSA release and hydrogel swelling. BSA (5 wt.%) was mixed with equal moles of IDA and metal ions in 10 wt.% PEGDA prepolymer solutions. The swelling ratios of each nondegradable gel were measured after protein release. $n = 3$, mean ± SD. Concentration of I-2959: 0.2 wt.%; *, **: statistically significant at $p < 0.05$.

Total release of BSA from all ligand-containing systems is significantly higher than when no ligand is present.

Figure 6 also shows the mass swelling ratio of the ligand-containing gels. The swelling ratio of all gels remains relatively constant and suggests that the cross-linking density of the hydrogel is not affected by the addition of IDA or any metal ions. Thus the observed, enhanced release of BSA is solely attributable to the association of BSA with IDA, and not to changes in gel cross-linking density and protein diffusivity.

The data in Fig. 6 further demonstrate a direct correlation between the extent of protein–ligand binding and protein release efficiency. The results presented in Fig. 3 demonstrate an inverse correlation between the extent of protein–ligand binding and the extent of protein–polymer coupling. Taken together, the results in Figs. 3 and 6 support the conclusion that BSA is protected from adverse side reactions with free radicals during gel formation by complexing with the small-molecule IDA ligand. The higher the fraction of protein bound to the ligand, the greater the observed increase in release efficiency. Although the addition of metal ions can be beneficial to the therapeutic efficacy when released *in vitro*, a potential problem behind this approach is the toxicity of metal ions *in vivo*. Nonetheless, the increased amount of protein delivery proved by this research does open an avenue for enhancing protein stability during hydrogel formation and protein encapsulation.

Prediction of Reversible IDA–BSA Binding

A theoretical prediction of the extent of BSA–IDA–Cu^{2+} association based on the binding equilibrium shown in Eqs. (1) and (2) is presented in Fig. 7. At equilibrium, binding between BSA and the IDA–Cu^{2+} complex is considered reversible and is determined, in part, by the K_d value and total BSA concentration. The degree of association decreases with K_d and increases with BSA concentration. BSA

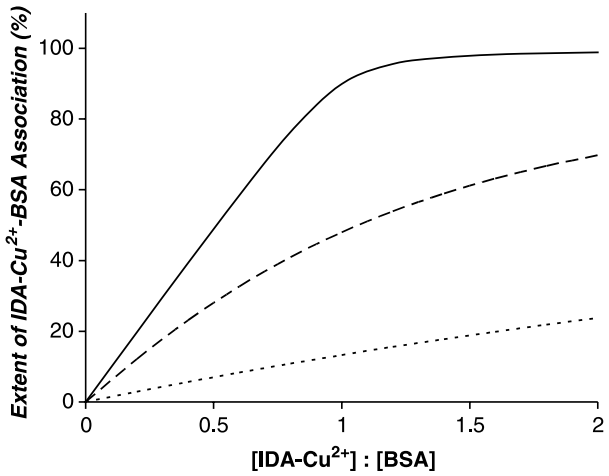

Fig. 7. Predicted extent of association between BSA and IDA–Cu^{2+} complex (K_d = 0.0082 mM) as a function of total protein concentration. Solid curve: 5 wt.% BSA; dashed curve: 0.5 wt.% BSA; dotted curve: 0.01 wt.% BSA. The extent of association is defined as the molar ratio of IDA–Cu^{2+}–BSA complex to unbounded BSA.

is far more concentrated in the prepolymer solution than in the swollen gel of the surrounding media. Furthermore, compared to the protein-rich hydrogel (50 μL), the relatively protein and ligand-free supernatant solution (5 mL) can be treated as a "sink" where the BSA concentration is dramatically lower than in the gel. In Fig. 7, the solid curve represents the theoretical extent of BSA–IDA–Cu^{2+} association present in a 5 wt.% BSA prepolymer solution at different BSA–IDA–Cu^{2+} molar ratios (K_d = 0.0082 mM). The extent of BSA–IDA–Cu^{2+} association is approximately 90% when a 1:1 molar ratio of IDA–Cu^{2+} to BSA is used. However, when BSA–IDA–Cu^{2+} complex is released from the hydrogel, its bulk concentration rapidly decreases. For example, under the same conditions, a drop in BSA concentration from 5% (solid curve) to 0.01% (dotted curve) also lowers the degree of association from 90% to only 13%. In other words, most of the released BSA will dissociate from the BSA– IDA–Cu^{2+} complex because of its diluted concentration and make BSA available to its target in its uncomplexed, native form. The general trends in BSA–IDA–Cu^{2+} binding shown in Fig. 7 can be readily extrapolated to other protein–ligand pairs.

Prediction of BSA Total Release

To further understand the mechanism of BSA protection provided by IDA–metal ion complexes during free-radical polymerization, a theoretical model was developed to predict total BSA release from gels where IDA-based ligands with different protein affinities are incorporated in the prepolymer solutions at various concentrations. The total release of BSA can be modeled by using known dissociation constant values and a single experimentally determined variable, the fraction of protein nonspecifically immobilized in the hydrogel (*i*). Figure 8 illustrates the ability of this model to predict total BSA release from systems exhibiting different protein affinities as well as ligand–protein ratios. The agreement between predictions of this theoretical model and experimental BSA release data shown in Fig. 8 support the proposed mechanism of BSA immobilization and IDA-mediated protection within the photopolymerized networks.

Once validated, the developed protein–ligand binding model can be used to explain experimental observations. As shown in Fig. 8, the total release of BSA depends upon the initial BSA loading concentration as well as the ligand–protein ratio. Recall from Fig. 2 that BSA total release increases with the protein loading concentration. Therefore, *i* values were obtained from the experimentally determined total BSA release at 10 and 5 wt.% in Fig. 2 and used to predict release at all ligand–protein ratios (dashed and solid lines) using Eq. (3).

From Eq. (3) it can be understood that the relatively weak binding affinity between BSA and IDA leading to low total BSA release can be countered by increasing IDA concentration. The increased ligand concentration forces the free protein into the associated protein–ligand state and therefore increases its degree of protection and total release. As shown by the solid line (model prediction) and open triangles (experimental data) in Fig. 8, when the molar ratio of IDA to BSA is increased to a ratio of 4:1, the total release of BSA is increased to almost 90% compared to only 45% when no IDA is used. As predicted by the model, further increasing the IDA concentration to a molar ratio of 10 does not significantly increase the total release of BSA (data not shown).

Total release of BSA also increases with initial BSA loading concentration. As shown by the dotted (10 wt.% loaded BSA) and dashed (5 wt.% loaded BSA) lines in Fig. 8, the more BSA loaded into the prepolymer solution, the greater its total fractional release. Additionally, the model predicts differences in total BSA release when a variety of protein–binding ligands are utilized. For example, incorpo-

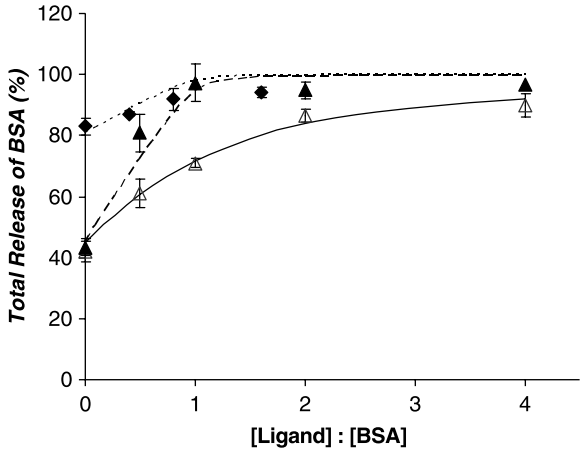

Fig. 8. Comparison of experimentally determined total BSA release (symbols) with predictions of a theoretical model (curves). Release data obtained with various molar ratios of ligand to protein are used to verify the accuracy of the model. Ligand–protein ratios, protein loading concentration, and ligand–protein affinity all affect total BSA release. Release data and predictions from three systems are compared: (a) IDA–Cu^{2+} with K_d = 0.0082 mM, $[BSA]_0$ = 10 wt.% (♦ and dotted curve); (b) IDA–Cu^{2+} with K_d = 0.0082 mM, $[BSA]_0$ = 5 wt.% (▲ and dashed curve); and (c) IDA alone with K_d = 0.4 mM and $[BSA]_0$ = 5 wt.% (△ and solid curve). *n* = 3, mean ± SD. Concentration of I-2959: 0.2 wt.%.

rating the IDA–Cu^{2+} ligand into a 5 wt.% BSA prepolymer solution leads to higher total BSA release values than incorporation of IDA alone at similar ligand–protein ratios (solid triangles *vs*. open triangles). This increase is attributable to the higher affinity of the IDA–Cu^{2+} complex for BSA compared to IDA. Release data from systems incorporating high concentrations of IDA–Cu^{2+} ligand are not obtained because high Cu^{2+} concentrations prevented gel formation.

Although the exact mechanism in which the IDA–Cu^{2+} complex provides a protection effect on BSA during polymer network formation remains undetermined, we speculate this protection effect is attributable to the fact that the copper-binding site on BSA also acts as a reactive center for protein–polymer conjugation as discussed previously. Therefore, when IDA–Cu^{2+} complex is added, immobilization of BSA to the cross-linked polymer network is reduced, which leads to an increased amount of BSA release. An alternative hypothesis is that binding of the IDA or IDA–Cu^{2+} complex to BSA leads to a change in protein conformation that hinders accessibility of free radicals to any number of reactive sites on the BSA surface.

Although the model can accurately predict the total release of BSA in the presence of IDA or IDA–Cu^{2+} complex, there are limitations to the model predictions. The model was developed under the assumption of a single IDA–Cu^{2+} binding site per BSA molecule. The binding equilibrium shown in Eqs. (1) and (2) is valid only when the single binding site assumption holds. Some research suggests, however, that a second, weaker copper binding site exists on BSA (43). It is also assumed that the BSA is present in a nonaggregated state. If BSA forms aggregates under certain unfavorable conditions, which is not the case in this study as shown in Fig. 3, the predicted binding equilibrium based on total protein concentration will not be valid. In the present model, purely empirical values for the model parameter i were used to generate the theoretical release curves only applicable to the system analyzed in this study. The amount of protein nonspecifically immobilized in the polymer networks will vary with external conditions such as the photopolymerization reaction parameters as well as inherent biochemical properties such as the extent of protein–polymer interaction. A method or model is needed to predict the amount of protein immobilized under specific photopolymerization conditions in the absence of protein-binding ligand. This is possible only when the exact mechanism of protein-free radical conjugation is resolved. Nevertheless, the results presented here demonstrate a possible mechanism of protein–polymer interaction and provide a solution that minimizes this undesired interaction.

CONCLUSIONS

The release efficiency of BSA from photopolymerized PEG hydrogels is increased by incorporating a soluble transition metal chelator (iminodiacetic acid) into the prepolymer solutions. The significance of this strategy is that the protein protection effect is achieved by simply adding IDA and metal ions while maintaining the advantages provided by *in situ* photopolymerization and simultaneous protein encapsulation. The undesired protein–radical interactions commonly observed during PEG hydrogel formation and the reduction in total protein release were minimized via ligand incorporation. Specifically, BSA release efficiency was enhanced by adding IDA and different transition metal ions to the prepolymer solution. Although BSA is used in this study, it is hypothesized that similar protection strategies can be applied to other therapeutically valuable proteins displaying an affinity for IDA. This includes proteins exhibiting transition metal binding domains such as hepatocyte growth factor (HGF) or human growth hormone (hGH) and recombinant proteins engineered with histidine tags (49). Furthermore, specialized ligands other than IDA can be engineered to display affinities for specific proteins of interest and thereby increase their release efficiency in a manner similar to that seen with BSA.

ACKNOWLEDGMENTS

The authors wish to acknowledge Drs. Sarah Harcum, James Morris, and Meredith Morris for discussion in SDS-PAGE. The project was supported in part by funding from NSF-EPSCoR.

REFERENCES

1. M. L. Vance and N. Mauras. Growth hormone therapy in adults and children. *N. Engl. J. Med.* **341**:1206–1216 (1999).
2. C. M. Dobson. Protein folding and misfolding. *Nature* **426**:884–890 (2003).
3. E. Y. Chi, S. Krishnan, T. W. Randolph, and J. F. Carpenter. Physical stability of proteins in aqueous solution: mechanism and driving forces in nonnative protein aggregation. *Pharm. Res.* **20**:1325–1336 (2003).
4. N. A. Peppas, K. B. Keys, M. Torres-Lugo, and A. M. Lowman. Poly(ethylene glycol)-containing hydrogels in drug delivery. *J. Control. Release* **62**:81–87 (1999).
5. L. M. Schwarte and N. A. Peppas. Novel poly(ethylene glycol)-grafted, cationic hydrogels: preparation, characterization and diffusive properties. *Polymer* **39**:6057–6066 (1998).
6. A. S. Sawhney, C. P. Pathak, and J. A. Hubbell. Bioerodible hydrogels based on photopolymerized poly(ethylene glycol)-*co*-poly(alpha-hydroxy acid) diacrylate macromers. *Macromolecules* **26**:581–587 (1993).
7. K. S. Anseth, A. T. Metters, S. J. Bryant, P. J. Martens, J. H. Elisseeff, and C. N. Bowman. *In situ* forming degradable networks and their application in tissue engineering and drug delivery. *J. Control. Release* **78**:199–209 (2002).
8. J. L. Drury and D. J. Mooney. Hydrogels for tissue engineering: scaffold design variables and applications. *Biomaterials* **24**:4337–4351 (2003).
9. Y. M. Ju, K. D. Ahn, J. M. Kim, J. A. Hubbell, and D. K. Han. Physical properties and biodegradation of lactide-based poly (ethylene glycol) polymer networks for tissue engineering. *Polym. Bull.* **50**:107–114 (2003).
10. K. T. Nguyen and J. L. West. Photopolymerizable hydrogels for tissue engineering applications. *Biomaterials* **23**:4307–4314 (2002).
11. K. H. Schmedlen, K. S. Masters, and J. L. West. Photocrosslinkable polyvinyl alcohol hydrogels that can be modified with cell adhesion peptides for use in tissue engineering. *Biomaterials* **23**:4325–4332 (2002).
12. Y. J. An and J. A. Hubbell. Intraarterial protein delivery via intimally-adherent bilayer hydrogels. *J. Control. Release* **64**:205–215 (2000).

13. B. Kim and N. A. Peppas. Poly(ethylene glycol)-containing hydrogels for oral protein delivery applications. *Biomed. Microdevices* **5**:333–341 (2003).
14. B. Kim and N. A. Peppas. *In vitro* release behavior and stability of insulin in complexation hydrogels as oral drug delivery carriers. *Int. J. Pharm.* **266**:29–37 (2003).
15. D. J. Quick and K. S. Anseth. Gene delivery in tissue engineering: a photopolymer platform to coencapsulate cells and plasmid DNA. *Pharm. Res.* **20**:1730–1737 (2003).
16. D. J. Quick and K. S. Anseth. DNA delivery from photocrosslinked PEG hydrogels: encapsulation efficiency, release profiles, and DNA quality. *J. Control. Release* **96**:341–351 (2004).
17. D. J. Quick, K. K. Macdonald, and K. S. Anseth. Delivering DNA from photocrosslinked, surface eroding polyanhydrides. *J. Control. Release* **97**:333–343 (2004).
18. G. Crotts and T. G. Park. Protein delivery from poly(lactic-*co*-glycolic acid) biodegradable microspheres: release kinetics and stability issues. *J. Microencapsul.* **15**:699–713 (1998).
19. W. R. Gombotz and D. K. Pettit. Biodegradable polymers for protein and peptide drug-delivery. *Bioconjug. Chem.* **6**:332–351 (1995).
20. M. Chiba, J. Hanes, and R. Langer. Controlled protein delivery from biodegradable tyrosine-containing poly(anhydride-*co*-imide) microspheres. *Biomaterials* **18**:893–901 (1997).
21. G. Jiang, B. H. Woo, F. R. Kang, J. Singh, and P. P. DeLuca. Assessment of protein release kinetics, stability and protein polymer interaction of lysozyme encapsulated poly (D,L-lactide-*co*-glycolide) microspheres. *J. Control. Release* **79**:137–145 (2002).
22. W. L. Jiang and S. P. Schwendeman. Stabilization of a model formalinized protein antigen encapsulated in poly(lactide-*co*-glycolide)-based microspheres. *J. Pharm. Sci.* **90**:1558–1569 (2001).
23. W. L. Jiang and S. P. Schwendeman. Stabilization and controlled release of bovine serum albumin encapsulated in poly(D,L-lactide) and poly(ethylene glycol) microsphere blends. *Pharm. Res.* **18**:878–885 (2001).
24. J. C. Kang and S. P. Schwendeman. Comparison of the effects of Mg(OH)(2) and sucrose on the stability of bovine serum albumin encapsulated in injectable poly(D,L-lactide-coglycolide) implants. *Biomaterials* **23**:239–245 (2002).
25. H. K. Kim and T. G. Park. Microencapsulation of human growth hormone within biodegradable polyester microspheres: protein aggregation stability and incomplete release mechanism. *Biotechnol. Bioeng.* **65**:659–667 (1999).
26. S. P. Schwendeman. Recent advances in the stabilization of proteins encapsulated in injectable PLGA delivery systems. *Crit. Rev. Ther. Drug Carrier Syst.* **19**:73–98 (2002).
27. G. Z. Zhu, S. R. Mallery, and S. P. Schwendeman. Stabilization of proteins encapsulated in injectable poly(lactide-*co*-glycolide). *Nat. Biotechnol.* **18**:52–57 (2000).
28. G. Z. Zhu and S. P. Schwendeman. Stabilization of proteins encapsulated in cylindrical poly(lactide-*co*-glycolide) implants: mechanism of stabilization by basic additives. *Pharm. Res.* **17**:351–357 (2000).
29. M. Belew and J. Porath. Immobilized metal-ion affinity-chromatography—effect of solute structure, ligand density and salt concentration on the retention of peptides. *J. Chromatogr.* **516**:333–354 (1990).
30. L. Nieba, S. E. NiebaAxmann, A. Persson, M. Hamalainen, F. Edebratt, A. Hansson, J. Lidholm, K. Magnusson, A. F. Karlsson, and A. Pluckthun. BIACORE analysis of histidine-tagged proteins using a chelating NTA sensor chip. *Anal. Biochem.* **252**:217–228 (1997).
31. J. Porath. Imac—immobilized metal-ion affinity based chromatography. *Trac-Trends Anal. Chem.* **7**:254–259 (1988).
32. E. P. Beers and J. Callis. Utility of polyhistidine-tagged ubiquitin in the purification of ubiquitin–protein conjugates and as an affinity ligand for the purification of ubiquitin-specific hydrolases. *J. Biol. Chem.* **268**:21645–21649 (1993).
33. C. H. Min and G. L. Verdine. Immobilized metal affinity chromatography of DNA. *Nucleic Acids Res.* **24**:3806–3810 (1996).
34. L. Schmitt, C. Dietrich, and R. Tampe. Synthesis and characterization of chelator-lipids for reversible immobilization of engineered proteins at self-assembled lipid interfaces. *J. Am. Chem. Soc.* **116**:8485–8491 (1994).
35. C. M. Zhang, S. A. Reslewic, and C. E. Glatz. Suitability of immobilized metal affinity chromatography for protein purification from canola. *Biotechnol. Bioeng.* **68**:52–58 (2000).
36. Q. Z. Luo, H. F. Zou, X. Z. Xiao, Z. Guo, L. Kong, and X. Q. Mao. Chromatographic separation of proteins on metal immobilized iminodiacetic acid-bound molded monolithic rods of macroporous poly(glycidyl methacrylate-*co*-ethylene dimethacrylate). *J. Chromatogr., A* **926**:255–264 (2001).
37. S. Sharma and G. P. Agarwal. Interactions of proteins with immobilized metal ions: a comparative analysis using various isotherm models. *Anal. Biochem.* **288**:126–140 (2001).
38. L. Yang, L. Y. Jia, H. F. Zou, and Y. K. Zhang. Immobilized iminodiacetic acid (IDA)-type Cu^{2+}-chelating membrane affinity chromatography for purification of bovine liver catalase. *Biomed. Chromatogr.* **13**:229–234 (1999).
39. C. Harford and B. Sarkar. Amino terminal Cu(II)- and Ni(II)-binding (ATCUN) motif of proteins and peptides: metal binding, DNA cleavage, and other properties. *Acc. Chem. Res.* **30**:123–130 (1997).
40. E. Hochuli, H. Dobeli, and A. Schacher. New metal chelate adsorbent selective for proteins and peptides containing neighboring histidine-residues. *J. Chromatogr.* **411**:177–184 (1987).
41. H. Iwata, K. Saito, S. Furusaki, T. Sugo, and J. Okamoto. Adsorption characteristics of an immobilized metal affinity membrane. *Biotechnol. Prog.* **7**:412–418 (1991).
42. E. Sulkowski. Purification of proteins by Imac. *Trends Biotechnol.* **3**:1–7 (1985).
43. Y. Zhang and D. E. Wilcox. Thermodynamic and spectroscopic study of Cu(II) and Ni(II) binding to bovine serum albumin. *J. Biol. Inorg. Chem.* **7**:327–337 (2002).
44. G. M. Cruise, O. D. Hegre, D. S. Scharp, and J. A. Hubbell. A sensitivity study of the key parameters in the interfacial photopolymerization of poly(ethylene glycol) diacrylate upon porcine islets. *Biotechnol. Bioeng.* **57**:655–665 (1998).
45. N. Kubota, Y. Nakagawa, and Y. Eguchi. Recovery of serum proteins using cellulosic affinity membrane modified by immobilization of Cu^{2+} ion. *J. Appl. Polym. Sci.* **62**:1153–1160 (1996).
46. J. Porath. Immobilized metal-ion affinity-chromatography. *Protein Expr. Purif.* **3**:263–281 (1992).
47. E. K. M. Ueda, P. W. Gout, and L. Morganti. Current and prospective applications of metal ion–protein binding. *J. Chromatogr., A* **988**:1–23 (2003).
48. T. T. Yip, Y. Nakagawa, and J. Porath. Evaluation of the interaction of peptides with Cu(II), Ni(II), and Zn(II) by high-performance immobilized metal-ion affinity-chromatography. *Anal. Biochem.* **183**:159–171 (1989).
49. N. Rahimi, S. Etchells, and B. Elliott. Hepatocyte growth factor (HGF) is a copper-binding protein: a facile probe for purification of HGF by immobilized Cu(II)-affinity chromatography. *Protein Expr. Purif.* **7**:329–333 (1996).